Material gain of bulk 1.55 μm InGaAsP/InP semiconductor optical amplifiers approximated by a polynomial model

J. Leuthold, M. Mayer, J. Eckner, G. Guekos, H. Melchior et al.

Citation: J. Appl. Phys. **87**, 618 (2000); doi: 10.1063/1.371909
View online: http://dx.doi.org/10.1063/1.371909
View Table of Contents: http://jap.aip.org/resource/1/JAPIAU/v87/i1
Published by the American Institute of Physics.

Material gain of bulk 1.55 μm InGaAsP/InP semiconductor optical amplifiers approximated by a polynomial model

J. Leuthold,[a] M. Mayer, J. Eckner, G. Guekos, and H. Melchior
Institute of Quantum Electronics, Swiss Federal Institute of Technology (ETH), CH-8093 Zürich, Switzerland

Ch. Zellweger
Institute of Micro- and Optoelectronics, Swiss Federal Institute of Technology (EPFL), CH-1015 Lausanne, Switzerland

(Received 5 April 1999; accepted for publication 5 October 1999)

We report material gain measurements of bulk 1.55 μm InGaAsP/InP performed at constant temperature and carried out over a large range of carrier densities and a large spectral region. In addition, a polynomial model for the material gain is proposed that not only fits the experimental data well over the whole measured range but also shows stable convergence in simulation tools when carrier densities exceed the usual range. To get reliable parameters for the model we eliminated temperature effects arising from different current biases and performed material-gain measurements over the largest possible carrier density range. The material-gain model realized is used in semiconductor optical amplifier simulation tools. © *2000 American Institute of Physics.* [S0021-8979(00)09301-4]

Semiconductor optical amplifier (SOA) device-simulation tools require detailed knowledge of the material gain g_m over a broad range of carrier injection densities N and wavelengths λ.[1,2] In addition, the optical gain is a key factor for the design of lasers and SOAs. However, theoretical calculation of the material gain $g_m(\lambda,N)$ is cumbersome, see, e.g. Refs. 3 and 4, and the match with experimental data is usually moderate. Therefore, different approximation formulas for the material gain have been proposed. Assuming that the SOA is a simple two-level system, the material gain has been modeled as having a symmetric Lorentzian line shape.[5] This approach is limited because the gain coefficient is asymmetric with the wavelength. In another attempt the experimentally determined curves were empirically fitted to a quadratic function.[6] While this function corresponds to the gain coefficient near the peak of the gain, it fails to give an adequate description especially on the long wavelength side. In order to more effectively model the asymmetric gain, Willner and Shieh proposed a cubic formula.[7] However, their parametrization is unsatisfactory in the short wavelength range.

Here we report on material-gain measurements of 1.55 μm InGaAsP/InP and we propose a polynomial approximation for the experimentally determined material gain. We show that the model predicts our measured temperature-controlled material gain curves well over all the measured range. The model is of special interest for use in simulation tools, since it delivers reasonable physical values even for unphysical high or low carrier densities that every now and again occur in simulation tools and that otherwise cause convergence problems. To the best or our knowledge, it is the only 1.55 μm InGaAsP/InP material-gain measurement over a large carrier density and spectral range at that precision.

The proposed model is the sum of a quadratic and a cubic function (see Fig. 1),

$$\overline{g_m}(\lambda,N) = \begin{cases} c_N[\lambda-\lambda_z(N)]^2+d_N[\lambda-\lambda_z(N)]^3, & \lambda<\lambda_z(N), \\ 0, & \lambda\geqslant\lambda_z(N), \end{cases} \tag{1}$$

with

$$c_N=3\,\frac{g_p(N)}{[\lambda_z(N)-\lambda_p(N)]^2}, \tag{2a}$$

$$d_N=2\,\frac{g_p(N)}{[\lambda_z(N)-\lambda_p(N)]^3}. \tag{2b}$$

The functions $g_p(N)$, $\lambda_p(N)$, and $\lambda_z(N)$ required in Eqs. (2a) and (2b) are the material gain versus carrier density at peak wavelength, the carrier dependence of the peak wavelength, and the wavelength at which the gain falls to zero for increasing λ at a given carrier density.

These functions have to be chosen such that they fulfill the physically reasonable conditions,

$$g_p(N)>0 \tag{3}$$

and

$$\lambda_z(N)>\lambda_p(N)$$

for all N.

Based on our experimental data we suggest approximating these functions by

$$g_p(N)=a_0(N-N_0)+\overline{a}a_0N_0e^{-N/N_0} \tag{4a}$$

$$\lambda_p(N)=\lambda_0-[b_0(N-N_0)+b_1(N-N_0)^2], \tag{4b}$$

[a]Now with Bell Labs, Lucent Technologies, Holmdel NJ 07733; electronic mail: leuthold@lucent.com

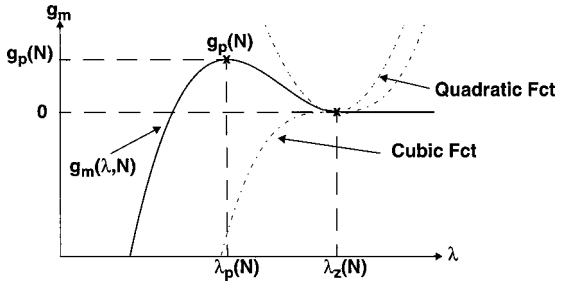

FIG. 1. Material gain $g_m(\lambda, N)$ modeled as the sum of a quadratic and a cubic function that have their zeros in λ_z. For determination of the polynomial function, we only need to know the carrier dependence of λ_z, λ_p, and g_p.

$$\lambda_z(N)=\lambda_{z_0}-z_0(N-N_0), \tag{4c}$$

where the coefficients N_0, a_0, $\overline{a}$, λ_0, b_0, b_1, λ_{z0}, and z_0 have to be determined from experiments. N_0 represents the transparency carrier density at the band edge wavelength λ_0 of the active layer and λ_{z_0} is the value of λ_z at the transparency carrier density. The last term in Eq. (4a) is used to adapt the model to experimental data for low carrier densities, i.e., in the absorption range.

In order to determine these coefficients for 1.55 μm InGaAsP we need to measure the material gains. To perform these measurements we used a double-heterostructure-laser diode (LD) with straight cleaved facets and a second double-heterostructure device tilted 10° from the cleave direction. The device with the tilted facets had facet reflectivities below 10^{-4} and therefore could be used as a SOA. The two devices have the same basic structure and geometry (Fig. 2) and they were processed on the same chip ~100 μm from each other. The layers were grown by metalorganic chemical vapor deposition (MOCVD) and the ridge was first dry etched and then wet etched. To obtain representative data, we characterized three more laser diodes and two more SOAs, where one of each kind was on another wafer. We present here only the results of the first mentioned diodes, since the results of the other diodes are similar except for a variation in the peak wavelength.

To find the material gain g_m we first experimentally determined the net-modal gain $\overline{g}$, which corresponds to the modal gain averaged over the whole device[3]

$$\overline{g}=\Gamma g_m-\alpha_{\text{tot}}, \tag{5}$$

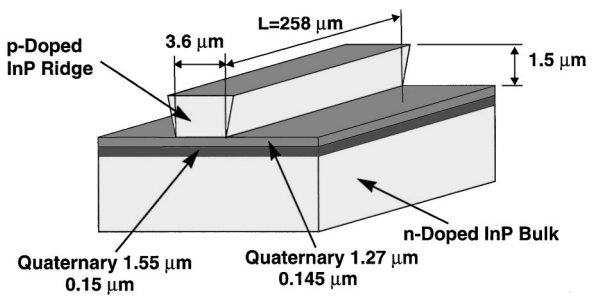

FIG. 2. Ridge-waveguide InGaAsP/InP laser and SOA structure used in our experiments.

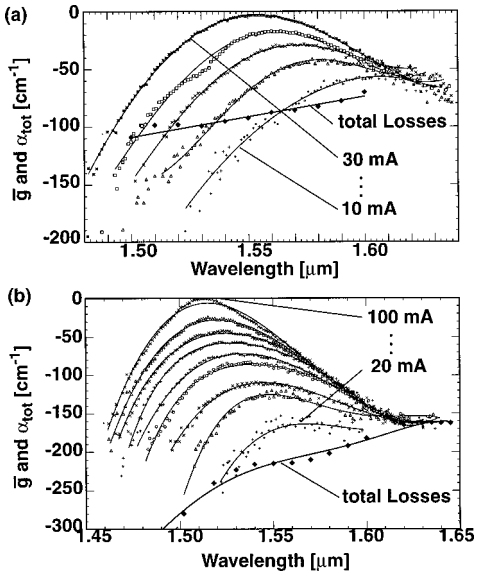

FIG. 3. Net-modal gain and total losses of (a) LD_1 for currents between 10 and 30 mA in steps of 5 mA and (b) SOA_1 for currents between 20 and 100 mA in steps of 10 mA. The SOA_1 cavity temperature is kept at $T_c = 20\,^{\circ}\text{C}$ for all currents. The solid lines are least square fits.

where Γ is the confinement factor and α_{tot} the total losses averaged over the whole device of length L. Once we had determined $\overline{g}$, we quantified the loss term α_{tot} and the confinement factor Γ to derive the material gain g_m.

The net-modal gain $\overline{g}$ was determined by the Hakki–Paoli[8] and the Cassidy[9] methods. These methods exploit the depth of the modulation introduced in the below threshold amplified spontaneous emission spectrum by the Fabry–Pérot resonance to extract $\overline{g}$. Since the LD's threshold is at 34 mA and the radiation shows ripples of good quality between 7 and 30 mA, we used it to determine $\overline{g}$ at lower carrier densities, i.e., between 10 and 30 mA. The SOA starts lasing around 100 mA. It was used to determine $\overline{g}$ between 30 and 100 mA, i.e., at higher carrier densities. Spectral net-modal gain curves measured at a diode-cavity temperature of 20 °C are depicted in Fig. 3.

The thermal resistance R_{therm} of the device and of the interface between the semiconductor and the copper heat sink mount causes heating of the active layer. Thus, the active layer temperature T_{act} deviates from the copper heat sink temperature T_{sens} by the amount of heat P_{heat} produced within the active layer,

$$T_{\text{act}}=T_{\text{sens}}+R_{\text{therm}}P_{\text{heat}}(I), \tag{6}$$

with $P_{\text{heat}}=IV(I)-2P_{\text{SpTot}}(I)$, where I is the current bias, V the voltage drop across the diode, and P_{SpTot} the total emitted spontaneous power through one facet. For R_{therm} we found values of 129 and 81 K/W for the LD and the SOA, respectively.[10] The quality of the temperature correction mechanism can be tested most easily above threshold. Above threshold the carrier densities are in principle clamped, so that temperature changes are the only sources for possible refractive index changes. We found for our devices that the refractive index changes disappear above threshold when temperature corrections are applied but that we have consid-

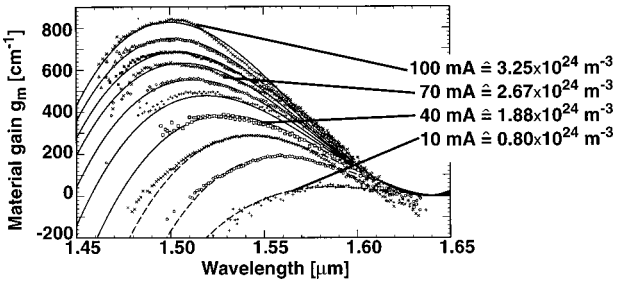

FIG. 4. Comparison of experimentally determined material gain (symbols) with material gain from the fit model (solid lines). The calculated curves fit the experimental data points well throughout the gain spectrum and for all carrier densities. The parametrized curves were calculated with Eq. (1) and the coefficients in the first column of Table I.

TABLE I. Coefficients for $In_{0.6}Ga_{0.4}As_{0.85}P_{0.15}$ polynomial models. (Wavelength units are in μm, carrier density units are in m^{-3}, and g_m is given in units of m^{-1}.)

Recommended parameters to use	In exact models	In simulation tools
Carrier density range allowed	$(N_0, \sim 4\times10^{24}\,m^{-3})$	$(0,\infty)$
N_0	$6.5\times10^{23}\,m^{-3}$	$6.5\times10^{23}\,m^{-3}$
a_0	$3.13\times10^{-20}\,m^2$	$3.13\times10^{-20}\,m^2$
$\overline{a}$	0	1.2
λ_0	1.595 μm	1.575 μm
b_0	$6.84\times10^{-26}\,m^3\,\mu m$	$3.17\times10^{-26}\,m^3\,\mu m$
b_1	$-1.22\times10^{-50}\,m^6\,\mu m$	0
λ_{z_0}	1.650 μm	1.625 μm
z_0	$5\times10^{-27}\,m^3\,\mu m$	$-2.5\times10^{-27}\,m^3\,\mu m$

erable refractive index changes when the temperature correction is not applied. Refractive index changes were detected by observation of the longitudinal mode shifts in the ripples of the spontaneous emission spectrum.[10,11]

Measured total losses α_{tot} are depicted in Fig. 3. Above the band gap energy they were measured by the transparency method[12,13] and below the band gap we used $\overline{g}=\alpha_{tot}$.

The confinement factor Γ was calculated for each wavelength with the help of a finite-element solver. Refractive index changes due to current bias changes were considered in the calculation.

The quaternary 1.55 μm material gain g_m at a cavity temperature of 20 °C is then obtained by insertion of $\overline{g}$, α_{tot}, and Γ into Eq. (5). The results are shown in Fig. 4.

The relationship between the carrier density N and the injection current I is needed in order to express the material properties with respect to the carrier densities. A convenient approach to determine $N(I)$ below threshold is based on the experimental determination of the differential carrier lifetime τ_d.[14,15] We applied this method to relate each current bias I with its respective carrier density N, given in the legend of Fig. 4.

Finally, we use the measured material-gain curves of Fig. 4 to determine the fit functions of Eqs. (4a)–(4c). Their coefficients are found by a least square fit to the experimental points at the peak maximum and at the band edge. The solid lines in Fig. 4, obtained with the coefficients from the first column in Table I, demonstrate the excellent agreement of our material-gain model over large parts of the measured ranges. With the coefficients in the second column of Table I we obtain a model, that fulfills the restrictions of Eq. (3) for all carrier densities between $(0,\infty)$. This model is of special interest for simulation tools, where occasionally unphysical values may occur, but the function must remain continuous in order to guarantee convergence. The model introduces small deviations from the measured curves in the low carrier density range due to the second term in Eq. (4a). In order to find material-gain models for other InGaAsP/InP layer compositions at the 1.5 μm band edge, it suffices to adjust the values λ_0 and λ_z.

In summary, we reported a simple polynomial fit function for material gain. The function correctly describes measured InGaAsP/InP material gains. The presented material-gain data are generally valid and are not bound to any specifically mounted device, since measurements were performed at a constant cavity temperature. The model and the data have been successfully used in the commercially available NM-SESES device solver for dynamic SOA investigations (Refs. 2, 16) and are currently being tested in the POSEIDON device simulation tool.[1]

R. Dall'Ara, from Opto-Speed SA in Lugano, Switzerland, is acknowledged for advice on the temperature correction mechanism.

[1] J. L. Pleumeekers, Ph.D. thesis, Delft University, 1997.
[2] E. Anderheggen, J. G. Korvink, M. Roos, G. Sartoris, and H. U. Schwarzenbach, NM-SESES, Numerical Modelling GmbH, Thalwil, Switzerland, 1996; http://www.nmtec.ch
[3] G. P. Agrawal and N. K. Dutta, *Long-Wavelength Semiconductor Lasers* (Van Nostrand Reinhold, New York, 1986).
[4] D. Gershoni, C. H. Henry, and G. A. Baraff, IEEE J. Quantum Electron. **29**, 2433 (1993).
[5] G. P. Agrawal, *Fiber-Optic Communication Systems* (Wiley, New York, 1992), Chap. 8.
[6] I. D. Henning, M. J. Adams, and J. V. Collins, IEEE J. Quantum Electron. **2**, 609 (1985).
[7] A. W. Willner and W. Shieh, J. Lightwave Technol. **13**, 771 (1995).
[8] B. W. Hakki and T. L. Paoli, J. Appl. Phys. **46**, 1299 (1975).
[9] D. T. Cassidy, J. Appl. Phys. **56**, 3096 (1984).
[10] J. Leuthold, *Series in Quantum Electronics* (Hartung–Gorre, Konstanz, Germany, 1999), Vol. 12.
[11] S. E. H. Turley, G. H. B. Thompson, and D. F. Lovelace, Electron. Lett. **15**, 256 (1979).
[12] K. A. Andrekson, N. A. Olsson, R. A. Logan, D. L. Coblenty, and H. Temkin, Electron. Lett. **28**, 171 (1992).
[13] G. E. Shtengel and D. A. Ackerman, Electron. Lett. **31**, 1157 (1995).
[14] W. Rideout, B. Yu, J. LaCourse, P. K. York, K. J. Beernink, and J. J. Coleman, Appl. Phys. Lett. **56**, 706 (1990).
[15] P. Granestrand, K. Fröjdh, O. Sahlén, B. Stoltz, and J. Wallin, Proceedings European Conference on Optical Communication 1998, p. 431.
[16] G. E. Sartoris and J. Leuthold, J. Modeling Simul. Microsyst. **1**, 1 (1999).